Journal of Molecular and Cellular Cardiology 60 (2013) 129–141

Contents lists available at SciVerse ScienceDirect

Journal of Molecular and Cellular Cardiology

journal homepage: www.elsevier.com/locate/yjmcc

Original article

Increased susceptibility of HIF-1α heterozygous-null mice to cardiovascular malformations associated with maternal diabetes

Romana Bohuslavova [a], Lada Skvorova [a], David Sedmera [b,c], Gregg L. Semenza [d,e,f], Gabriela Pavlinkova [a,*]

[a] Institute of Biotechnology AS CR, Prague, Czech Republic
[b] Institute of Anatomy, First Faculty of Medicine, Charles University, Prague, Czech Republic
[c] Institute of Physiology AS CR, Prague, Czech Republic
[d] Vascular Program, Institute for Cell Engineering, The Johns Hopkins University School of Medicine, Baltimore, MD, USA
[e] Departments of Pediatrics, Medicine, Oncology, Radiation Oncology, and Biological Chemistry, The Johns Hopkins University School of Medicine, Baltimore, MD, USA
[f] McKusick-Nathans Institute of Genetic Medicine, The Johns Hopkins University School of Medicine, Baltimore, MD, USA

ARTICLE INFO

Article history:
Received 1 September 2012
Received in revised form 13 April 2013
Accepted 15 April 2013
Available online 22 April 2013

Keywords:
Diabetic embryopathy
Heart defect
Hypoxia-inducible factor 1 alpha

ABSTRACT

Cardiovascular malformations are the most common manifestation of diabetic embryopathy. The molecular mechanisms underlying the teratogenic effect of maternal diabetes have not been fully elucidated. Using genome-wide expression profiling, we previously demonstrated that exposure to maternal diabetes resulted in dysregulation of the hypoxia-inducible factor 1 (HIF-1) pathway in the developing embryo. We thus considered a possible link between HIF-1-regulated pathways and the development of congenital malformations. HIF-1α heterozygous-null (Hif1a$^{+/-}$) and wild type (Wt) littermate embryos were exposed to the intrauterine environment of a diabetic mother to analyze the frequency and morphology of congenital defects, and assess gene expression changes in Wt and *Hif1a*$^{+/-}$ embryos. We observed a decreased number of embryos per litter and an increased incidence of heart malformations, including atrioventricular septal defects and reduced myocardial mass, in diabetes-exposed *Hif1a*$^{+/-}$ embryos as compared to Wt embryos. We also detected significant differences in the expression of key cardiac transcription factors, including Nkx2.5, Tbx5, and Mef2C, in diabetes-exposed Hif1a$^{+/-}$ embryonic hearts compared to Wt littermates. Thus, partial global HIF-1α deficiency alters gene expression in the developing heart and increases susceptibility to congenital defects in a mouse model of diabetic pregnancy.

1. Introduction

Diabetic pregnancy is associated with an increased incidence of congenital malformations compared with non-diabetic pregnancy [1,2]. Diabetic embryopathy can affect any developing organ system, although congenital heart defects are the most frequent malformations in the offspring of diabetic women [1]. Atrioventricular septal (AVS) defects, hypoplastic left heart syndrome, and persistent truncus arteriosus are the most frequent cardiac malformations detected in clinical studies [1,3–5]. The same types of heart malformations that are associated with diabetic pregnancies in humans have been reported in animal models [4,6–8]. Animal studies have indicated that hyperglycemia, hypoxia, fetal acidemia, and abnormal maternal/fetal fuel metabolism are responsible for changes in embryonic development [9–15]. Recent studies suggest that a major teratogenic effect of the diabetic-hyperglycemic milieu is mediated by increased oxidative stress and that administration of anti-oxidants reduces the occurrence of developmental defects [13–16]. However, the molecular mechanisms by which hyperglycemia or oxidative stress lead to the dysregulated gene expression that ultimately results in malformations have not yet been elucidated.

Using global gene expression profiling, we previously showed that maternal diabetes alters embryonic gene expression [17,18]. In particular, twenty genes regulated by hypoxia-inducible factor 1 (HIF-1) exhibited increased expression in diabetes-exposed embryos at E10.5, possibly reflecting an adaptive embryonic response to the diabetic environment of increased oxidative stress and hypoxia [17]. HIF-1 activates over 800 target genes that are involved in cell proliferation, angiogenesis, erythropoiesis, metabolism, and apoptosis [19]. Like other essential regulatory proteins, the expression levels of HIF-1 are highly controlled through the combinations of transcriptional, post-transcriptional, and post-translational mechanisms, and further influenced by protein stability and transactivation processes [19,42]. Oxygen tension plays a key role in the regulation of HIF-1α expression, stabilization, and activation [19]. The amplitude of this response is also modulated by growth factor and cytokine-dependent signaling pathways [20,21]. Furthermore, emerging evidence indicates that mitochondrial reactive oxygen species (ROS) are both necessary and sufficient to initiate the

* Corresponding author at: Laboratory of Molecular Pathogenetics, Institute of Biotechnology AS CR, v.v.i., Vídenská 1083, Prague 4, CZ-142 20, Czech Republic. Tel.: +420 241 063 415; fax: +420 244 471 707.
E-mail address: gpavlinkova@img.cas.cz (G. Pavlinkova).

0022-2828/$ – see front matter © 2013 Elsevier Ltd. All rights reserved.
http://dx.doi.org/10.1016/j.yjmcc.2013.04.015

stabilization and activation of HIF-1α, and that treatment with antioxidants prevents HIF-1α protein stabilization [22].

The critical role of HIF-1 in development is demonstrated by the consequences of homozygosity for a null allele at the *Hif1a* locus encoding the HIF-1α subunit. *Hif1a*$^{-/-}$ knockout mouse embryos die at mid-gestation due to cardiovascular and neural tube defects [23,24]. HIF-1α is essential for proper cardiac looping and the modulation of neural crest cell (NCC) migration and survival [24,25]. Interestingly, exposure of mouse embryos to increased ambient O_2 concentrations partially rescues development of the *Hif1a*$^{-/-}$ embryonic heart, specifically chamber formation. However, hyperoxia fails to rescue pharyngeal arch development and NCC migration. Furthermore, mice with global heterozygous deletion of HIF-1α concomitant with a cardiac specific homozygous deletion of HIF-1α in ventricular cardiomyocytes exhibit embryonic lethality due to abnormal cardiac development between E8.5 and E10.0 [26]. The global nature of the HIF-1α deletion in these studies does not allow a definitive attribution of the noted effects to a single cell type. Not only HIF-1α loss-of-function, but also excessive HIF-1 activity, may result in birth defects. CITED2 is a negative regulator of HIF-1 transcriptional activity and *Cited2*$^{-/-}$ mouse embryos manifest overexpression of HIF-1 target genes, such as *Vegfa*, *Glut1*, and *Pgk1*, as well as neural tube and cardiovascular defects [27]. Cardiac defects were partially rescued in *Cited2*$^{-/-}$;*Hif1a*$^{+/-}$ embryos [28]. Localized adenoviral overexpression of HIF-1α in the chick heart was sufficient to cause coronary artery anomalies [29]. Thus, increased or decreased HIF-1 activity results in neural and cardiovascular defects, which are the most frequent developmental defects associated with diabetic embryopathy.

Based on our finding that the expression of HIF-1 target genes is induced by maternal diabetes [17], and the knowledge that *Hif1a*$^{-/-}$ embryos have major defects in cardiovascular development [23,24], we hypothesized that HIF-1 transcriptional activity represents a protective response of the embryo to maternal diabetes and that loss of HIF-1 activity increases susceptibility to heart defects observed in diabetic embryopathy. *Hif1a*$^{+/-}$ heterozygous-null mice develop normally but demonstrate impaired responses when challenged with hypoxia after birth [30,31]. We hypothesized that limiting levels of HIF-1α may compromise embryonic development under conditions of aggravated hypoxia, which may occur in the context of maternal diabetes. We tested this hypothesis by exposing *Hif1a*$^{+/-}$ embryos to maternal diabetes. We analyzed the frequency and morphology of heart defects in diabetes-exposed *Hif1a*$^{+/-}$ and wild type (*Wt*) littermate embryos. Our results suggest an important role for HIF-1 in embryonic responses to the diabetic environment, including regulation of the key cardiac transcription factors *Nkx2.5*, *Tbx5*, and *Mef2C*.

2. Methods

2.1. Experimental animals

This study was conducted in accordance with the Guide for the Care and Use of Laboratory Animals (NIH Publication No. 85-23, revised 1996). Diabetes was induced in female inbred FVB mouse strain (strain code 207, Charles River), aged 7–9 weeks, by 2 intraperitoneal injections of 100 mg/kg body weight of streptozotocin (STZ; Sigma, St. Louis, MO), as described [17]. Blood glucose levels were measured in fasted animals by glucometer (COUNTOUR TS, Bayer, Switzerland). We analyzed embryos from 52 diabetic dams that maintained blood glucose levels above 13.9 mmol/L (classified as diabetic) with blood glucose levels (mean ± SD) of 10.0 ± 1.2; 18.3 ± 4.3; and 28.7 ± 6.36 mmol/L before STZ treatment, on the mating day, and at embryo harvest, respectively. Mouse embryos were isolated from diabetic or control dams between E10.5 and E18.5. Noon of the day on which the vaginal plug was found was designated E0.5. Diabetic FVB *Wt* females were mated to *Hif1a*$^{+/-}$ males (with the *Hif1a*^{tm1jhu} knockout allele [23] on an FVB background) to generate *Hif1a*$^{+/-}$ and *Wt* (*Hif1a*$^{+/+}$) littermate embryos. *Hif1a*$^{+/-}$ mice are defective in the induction of HIF-1α protein in response to hypoxia or ischemia [32,33]. Offspring of *Wt* × *Hif1a*$^{+/-}$ matings were genotyped by PCR [23,34]. Non-diabetic embryos were generated from crosses between mock-induced *Wt* females (i.e. no STZ treatment) to *Hif1a*$^{+/-}$ males. This breeding scheme minimized the potential influence of maternal genotype since the mutant allele was paternally contributed. The developmental stage was classified for each embryo by morphological criteria, including somite number as well as central nervous system, limb, and eye development. Embryonic and cardiac morphology was assessed using a Nikon SMZ dissection microscope. Digital images of whole embryos were captured with a Nikon DS-Fi1 camera. Measurements of the crown-rump length and relative heart area were obtained ex vivo by light microscopy using the NIS-elements software program (Nikon). We analyzed embryos that were comparable in their developmental progression.

2.2. Morphological analysis and immunostaining

Dissected thoraxes from E14.5 embryos were fixed with 4% paraformaldehyde in PBS (pH 7.4) at 4 °C overnight, dehydrated, and embedded in paraffin. Quantification of myocardial tissue area (ventricular compact myocardium and trabeculae) and the area of the ventricular lumens was performed in *Wt* and *Hif1a*$^{+/-}$ diabetes-exposed and control hearts (n = 5 each) using the threshold tool in the NIH ImageJ program (http://imagej.nih.gov/ij/download.html), as described [35]. We analyzed 3 consecutive sections of 7-μm thickness running through the atrioventricular (AV) junction with a four-chamber view. Immunohistochemistry was performed with anti-VEGF-A antibody at 1:50 dilution (#sc-7269, Santa Cruz Biotechnology, CA, USA), anti-α-smooth muscle actin (α-SMA) antibody at 1:500 dilution (#A2547, Sigma-Aldrich), and anti-phospho-histone H3 (pHH3) antibody (#06-570; Merck Millipore, Germany) at dilution 1:100; each analysis was repeated a minimum of 3 times on an average of 3 embryos per genotype and included appropriate controls. The sections were analyzed under a Nikon Eclipse 50i microscope with a 20× magnification objective using the NIS-element program. α-SMA and pHH3 immunostaining was analyzed with a two-photon microscope (Zeiss MP7). VEGF-A expression and α-SMA expression were quantified using ImageJ software. Immunopositive pHH3^{+} nuclei in compact myocardium were counted using Adobe Photoshop CS5.11.

2.3. TUNEL assay

For diabetes-exposed and control *Wt* and *Hif1a*$^{+/-}$ embryos, we analyzed 3 cardiac sections running through the AV junction with a four chamber view from 3 embryos of different litters for each genotype. Tissue sections (7 μm) of dissected E14.5 thoraxes were treated with 20 μg/ml proteinase K for 20 min at room temperature. The sections were incubated with the TUNEL labeling kit (Roche) for 1 h at 37 °C and Hoechst 33342 was used as a nuclear counterstain. The sections were analyzed under a Nikon Eclipse E400 fluorescent microscope.

2.4. Real-time reverse-transcription quantitative PCR

Total RNA was isolated from hearts at E14.5 from experimental samples (EXP; diabetes-exposed *Wt*, diabetes-exposed *Hif1a*$^{+/-}$, and non-diabetic *Hif1a*$^{+/-}$) and from non-diabetic *Wt* (control). Following reverse transcription (RT), quantitative real-time PCR (qPCR) was performed with the initial AmpliTaq activation at 95 °C for 10 min, followed by 40 cycles at 95 °C for 15 s and 60 °C for 60 s, as described [34]. The *Hprt1* gene was selected as the best reference gene for our analyses from a panel of 12 control genes (TATAA Biocenter AB, Sweden). The relative expression of a target gene was calculated, based on qPCR efficiencies (E) and the crossing point (Cp) difference (Δ) of an experimental sample versus control (ratio = $(E_{\text{target}})^{\Delta Cp\ \text{Gene(Mean control} - \text{Mean EXP)}}$ /

$(E_{\text{Hprt1}})^{\Delta\text{Cp Hprt1(Mean control} - \text{Mean EXP)}}$) [36]. RT-qPCR data were analyzed using the GenEX5 program (http://www.multid.se/genex/). Primer sets were designed to exclude amplification of potentially contaminating genomic DNA by positioning the amplicons across exon–exon junctions. Primers were designed using Primer 3 software (http://frodo.wi.mit.edu/primer3/). Primers were selected according to the following parameters: length between 18 and 30 bases; melting temperature (Tm) between 58° and 60 °C; and G + C content between 40 and 60% (optimal 50%). Primer sequences are presented in Supplemental Table S1.

2.5. Western blotting

Western blotting was performed according to a standard protocol using a monoclonal antibody that specifically recognizes HIF-1α [23]. Dissected E10.5 whole embryos without hearts and E10.5 hearts were lysed and stored at −80 °C until analysis. Protein levels were quantified using the BCA assay. Protein samples (25 μg per lane for whole embryos; 8 μg per lane for embryonic hearts) were denatured, resolved using 8% SDS-PAGE, and transferred onto a nitrocellulose membrane. The membrane was blocked with 5% dry milk and incubated overnight with anti-HIF-1α IgG in TBS buffer at 1:750 dilution (#NB100-105; Novus Biologicals, Cambridge, UK). Anti-β-actin IgG (#5125; Cell Signaling) was used as a loading control. After incubation with a horseradish peroxidase–conjugated secondary IgG (Amersham, IL, USA), the blots were developed using the SuperSignal* West Dura Chemiluminescent Substrate (Thermo Scientific, MI, USA). Chemiluminescent signals were captured using ImageQuant LAS 4000 Imager (GE Healthcare Bio-Sciences AB, Sweden) and analyzed by ImageJ software.

2.6. Statistical analysis

Fisher's exact test was used to compare the number of embryos and number of defects between two independent groups. A one-way analysis of variance (ANOVA) was used to investigate statistically significant differences among genotypes and experimental conditions. When a significant interaction was detected, the differences between subgroups were further compared using the post *t*-test (significance assigned at the $P < 0.05$ level; Graph Pad, 2005; Graph Pad, CA, USA).

3. Results

3.1. Effects of diabetes-exposure on litter size, embryonic growth, and external morphology of *Hif1a*$^{+/-}$ and Wt mice

Wt (n = 195) and *Hif1a*$^{+/-}$ (n = 163) embryos from 52 diabetic pregnancies, and *Wt* (n = 120) and *Hif1a*$^{+/-}$ (n = 117) embryos from 29 non-diabetic pregnancies were collected between E10.5 and E18.5 (Supplemental Table S2). The number of resorbed embryos was significantly increased in diabetic pregnancies with severe hyperglycemia (blood glucose level > 30 mmol/L; 24% of embryos) compared to non-diabetic pregnancies (2% of embryos) or diabetic pregnancies with blood glucose levels <30 mmol/L (3% of embryos). The average number of *Wt* embryos per litter was not significantly different in diabetic pregnancies with glucose levels >30 mmol/L (severe hyperglycemia; 3.97 ± 0.4) and in diabetic pregnancies with blood glucose levels between 13.9 mmol/L and 30 mmol/L (moderate hyperglycemia; 3.37 ± 0.4) compared to non-diabetic pregnancies (4.1 ± 0.4; Fig. 1). However, compared to *Wt* non-diabetic pregnancies, the number of *Hif1a*$^{+/-}$ embryos per litter was significantly lower in diabetic pregnancies with moderate hyperglycemia (3.28 ± 0.4; $P < 0.05$) or with severe hyperglycemia (3.05 ± 0.3; $P < 0.001$) (one-way ANOVA followed by Bonferroni post-test). The number of *Hif1a*$^{+/-}$ embryos per litter (3.1 ± 1.9) was significantly lower than *Wt* littermates in diabetic pregnancies (3.7 ± 1.7; $P < 0.05$).

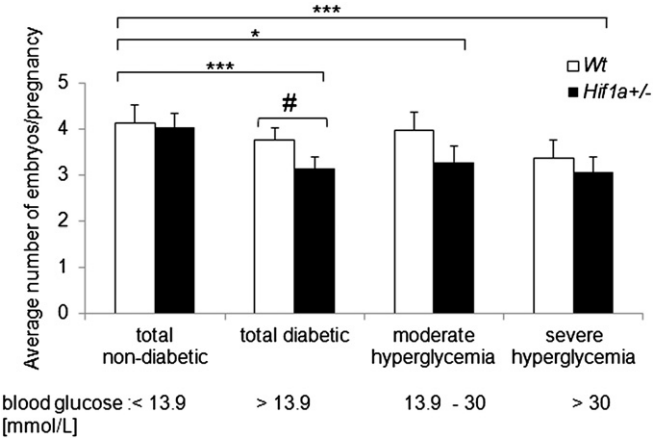

Fig. 1. Average number of embryos per litter. The average number of embryos per diabetic pregnancies (n = 52) was compared to non-diabetic pregnancies (n = 29). The number of *Wt* embryos/pregnancies was not affected by maternal diabetes in diabetic pregnancies with glucose levels >30 mmol/L (severe hyperglycemia; n = 18 litters) or in diabetic pregnancies with blood glucose levels between 13.9 mmol/L and 30 mmol/L (moderate hyperglycemia; n = 34 litters). The number of *Hif1a*$^{+/-}$ embryos/litter was significantly decreased in diabetic pregnancies compared to non-diabetic pregnancies. Statistical significance was assessed by one-way ANOVA (brackets at top) followed by Dunnett's post-test (all groups vs. non-diabetic *Wt* group). The values represent means ± SEM. *, $P < 0.05$; ***, $P < 0.001$; #, $P < 0.037$, *t-test*.

We detected a significant decrease in the average crown-rump length of *Wt* and *Hif1a*$^{+/-}$ diabetic embryos at E18.5 ($P < 0.0001$, one-way ANOVA; Supplemental Fig. S1A). The heart size of embryos from diabetic pregnancies was smaller than the sizes of embryonic hearts from non-diabetic pregnancies at E18.5 ($P < 0.0002$; Supplemental Fig. S1B).

Dissected embryos were examined for defects in gross morphology (Table 1). Diabetes-exposed embryos displayed a variety of external developmental defects, including neural tube defects and cardiovascular anomalies (Figs. 2A–J). Cardiovascular anomalies were the most frequent and were manifested by hemorrhage, edema, and in some cases, anemia. The evaluation of external phenotype of diabetes-exposed embryos demonstrated that *Hif1a*$^{+/-}$ embryos from diabetic pregnancies had an increased incidence of developmental defects of 22% (36 of 163) compared to 13% (26 of 195) of *Wt* littermate embryos (Fig. 2K; $P = 0.03$, Fisher's exact test). No significant effect of genotype on the frequency of developmental defects was detected in pregnancies with glucose levels >30 mmol/L (severe hyperglycemia) with frequencies of 26% (15 of 58) and 28% (18 of 64) for *Hif1a*$^{+/-}$ and *Wt* embryos, respectively ($P = 0.8$, Fisher's exact test). However, a significant effect of genotype on the incidence of developmental defects was observed

Table 1
Changes in gross morphology of diabetes-exposed embryos.

External developmental defects	*Wt* (n = 195)	*Hif1a*$^{+/-}$ (n = 163)
NTD[a]	2	5
NTD in the brain region/exencephaly	1	
NTD in the posterior region/spina bifida		2
Zig-zag closure	1	3
Combination of NTD and cardiovascular anomalies[b]	7	3
NTD in the brain region/exencephaly	5	1
Anencephaly	1	
NTD in the posterior region/spina bifida	2	1
Craniorachischisis		1
Caudal regression	1	2
Cardiovascular anomalies[b]	10	18
Developmental arrest	6	8

[a] NTD, neural tube defects.
[b] Cardiovascular anomalies were mostly manifested by hemorrhages and edema.

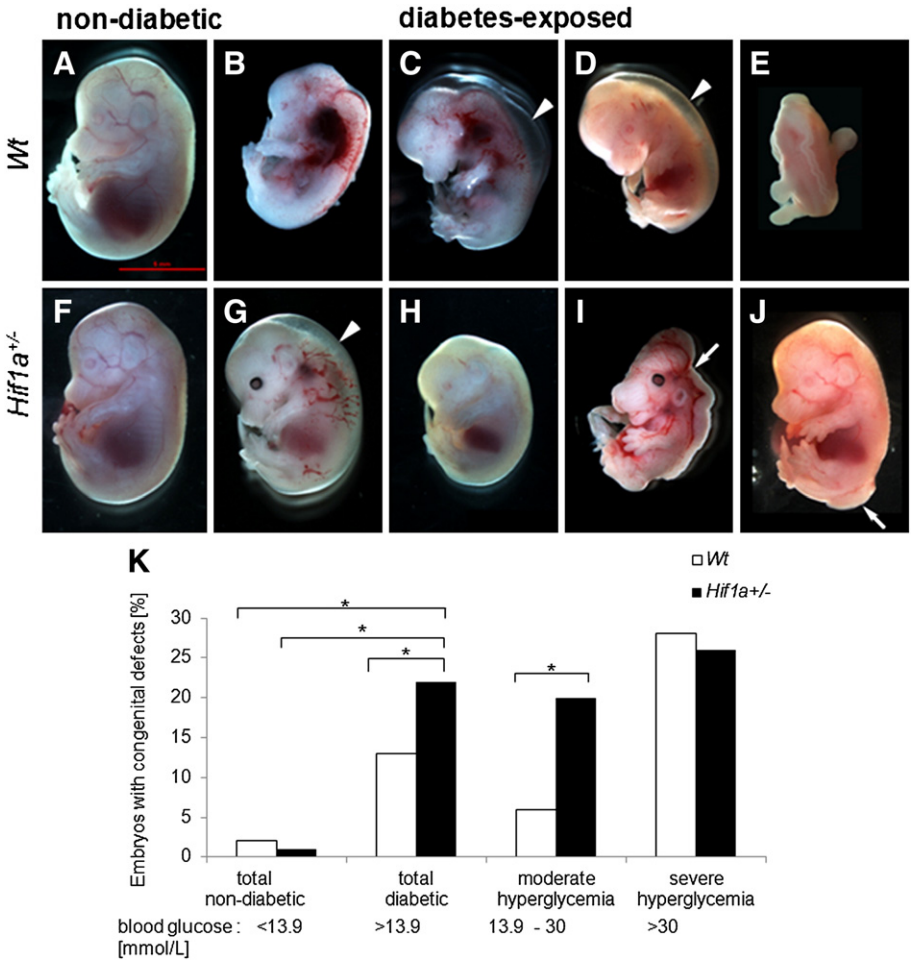

Fig. 2. External morphological changes in diabetes-exposed embryos at E14.5. The external appearances of *Wt* and *Hif1a*$^{+/-}$ embryos from non-diabetic (A, F) and diabetic pregnancies are compared at E14.5 (B–E, G–J). The most frequent defects associated with diabetic pregnancies were cardiovascular anomalies and neural tube defects. Neural tube defects were displayed mainly as neural tube closure defects (arrow in *J* and *I*) and in some cases as a phenotype of zig-zag closure line of neural tube (E). Cardiovascular anomalies were manifested by hemorrhages (B, C, G, I), edema (C, D, G, arrow head), and anemic phenotype in live embryos (H). Scale bar: 5 mm. (K): Incidence of congenital defects in embryos between E10.5 and E18.5 was affected by maternal diabetes. *Hif1a*$^{+/-}$ embryos from diabetic pregnancies (blood glucose levels > 13.9 mmol/L) showed an increased rate of congenital malformations of 22% (n = 36 of 163) compared to 13% of diabetes-exposed *Wt* (n = 26 of 195; $P = 0.03$, Fisher's exact test) and to 1% of non-diabetic *Hif1a*$^{+/-}$ embryos (n = 1 of 117; $P = 0.0001$, Fisher's exact test). No significant effect of genotype on the incidence of congenital defects was detected in diabetic pregnancies with glucose levels >30 mmol/L (severe hyperglycemia) with frequencies of 26% (n = 15 of 58) and 28% (n = 18 of 64; $P = 0.8$, Fisher's exact test) for *Hif1a*$^{+/-}$ and *Wt* embryos, respectively. However, the significant effect of genotype on the incidence of congenital defects was found in diabetic pregnancies with blood glucose levels between 13.9 mmol/L and 30 mmol/L (moderate hyperglycemia), in which 20% of *Hif1a*$^{+/-}$ embryos (n = 21 of 105) compared to 6% of *Wt* embryos (n = 8 of 131, $P = 0.002$, Fisher's exact test) demonstrated congenital defects. *, $P < 0.03$, Fisher's exact test.

in diabetic pregnancies with blood glucose levels of moderate hyperglycemia, in which 20% (21 of 105) of *Hif1a*$^{+/-}$ embryos, compared to only 6% (8 of 131) of *Wt* embryos, demonstrated developmental defects ($P = 0.002$, Fisher's exact test). Since we detected a significant effect of genotype on the incidence of developmental defects in embryos from diabetic pregnancies with moderate hyperglycemia, we used only embryos from pregnancies with moderate hyperglycemia for our subsequent analyses.

3.2. The frequency and morphology of cardiovascular defects

To assess the morphology and frequency of cardiovascular defects, we examined heart development and heart morphology by histological analysis of thorax sections of E14.5 embryos (Figs. 3A–D). Since HIF-1α modulates NCC survival and migration [25], we have carefully analyzed morphology of the outflow tract and pharyngeal arch arteries, because NCCs contribute to their formation. We analyzed 6 litters from diabetic dams consisting of 17 *Hif1a*$^{+/-}$ and 18 *Wt* embryos and 4 litters from non-diabetic dams consisting of 13 *Hif1a*$^{+/-}$ and 15 *Wt* embryos. The *Hif1a*$^{+/-}$ embryos from diabetic pregnancies showed an increased incidence of cardiovascular defects of 47% (n = 8 with defects/17 embryos; $P = 0.004$, Fisher's exact test) and *Wt* diabetes-exposed embryos showed an increased incidence of cardiac malformations of 28% (n = 5 with defects/18 embryos; $P = 0.048$, Fisher's exact test) compared to *Hif1a*$^{+/-}$ and *Wt* embryos from non-diabetic pregnancies, respectively. The majority of heart defects associated with diabetic pregnancy were AVS defects (65% of cardiovascular defects). We also identified pericardial effusion (12% of cardiac defects) in association with AVS defects.

We closely observed the cardiovascular malformations involving cardiac outflow tract defects. In 35 analyzed *Hif1a*$^{+/-}$ and *Wt* embryos from diabetic pregnancies, we identified one case of persistent truncus arteriosus in a *Hif1a*$^{+/-}$ embryo. We did not observe any cases of transposition of the great vessels or double outlet right ventricle. However, histological analysis showed that ventricular myocardial mass was profoundly reduced and the compact ventricular myocardial walls were thinner in all diabetes-exposed embryos at E14.5 (Figs. 3A–D, E; one-way ANOVA, $P < 0.0001$). Additionally, in diabetic pregnancies, the myocardial volume of the left ventricle (LV) of *Hif1a*$^{+/-}$ embryos was significantly decreased compared to *Wt* littermates (Fig. 3E). Interestingly, a sponge-like layer of myocardium (trabeculae) was increased in both diabetes-exposed *Wt* and *Hif1a*$^{+/-}$ embryos compared to non-diabetic *Wt* embryos (Fig. 3F). Since the ventricular trabeculae

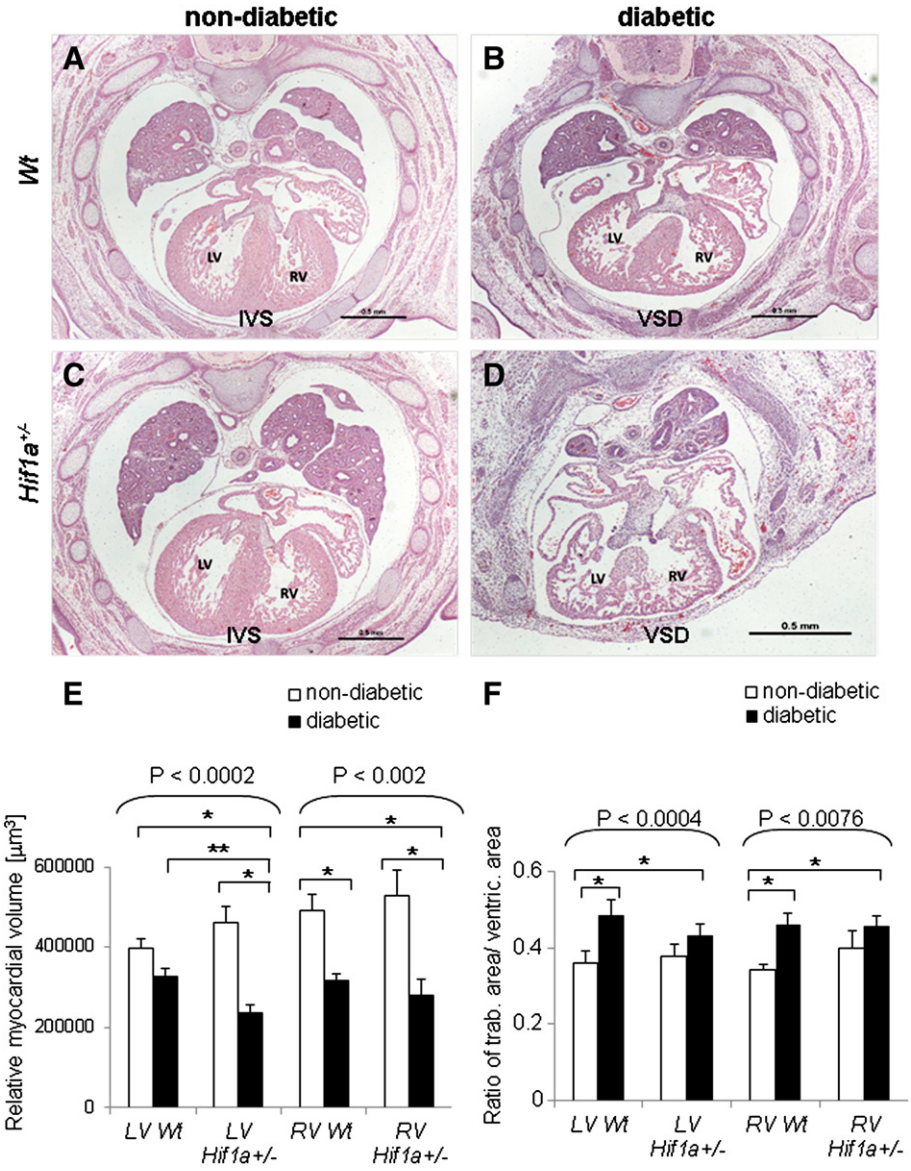

Fig. 3. Morphological changes in embryos exposed to maternal diabetes. H&E staining of mouse embryonic transverse sections of E14.5 thorax demonstrated an increased rate of cardiovascular defects in diabetes-exposed embryos (A–D). In *Wt* (A) and *Hif1a*$^{+/-}$ (C) embryos from non-diabetic pregnancies, the right and left ventricles were separated by the interventricular septum (IVS). In diabetes-exposed embryos (B, D), the 65% of detected cardiovascular defects were ventricular septal defects (VSD). Ventricular myocardial walls were thinner in all diabetes-exposed compared to non-diabetic embryos at E14.5. Scale bar: 0.5 mm. RV, right ventricle; LV, left ventricle; IVS, interventricular septum; VSD, ventricular septal defect. (E) The relative myocardial volumes (µm^3) of compact layer of diabetes-exposed RV of *Wt* ($P < 0.003$), RV of *Hif1a*$^{+/-}$ ($P < 0.01$), and LV of *Hif1a*$^{+/-}$ ($P < 0.001$) were significantly smaller compared to non-diabetic *Wt* and *Hif1a*$^{+/-}$ hearts. The compact myocardium of diabetes-exposed *Hif1a*$^{+/-}$ LV was significantly more affected than diabetes-exposed *Wt* LV ($P < 0.01$). The relative myocardial volume of compact layer (µm^3) was estimated from the areas of LV with length of 0.2 mm and RV with the length of 0.4 mm (µm^2) multiplied by the thickness of sections (7 µm). (F) Thickness of trabecular myocardium at E14.5. The average area of trabecular myocardium of both the LV ($P < 0.0004$) and RV ($P < 0.0076$) was significantly increased in the diabetes-exposed hearts of *Wt* and *Hif1a*$^{+/-}$ embryos compared to non-diabetic *Wt*. Ventricular trabecular area was quantified using ImageJ software. We analyzed compact and trabecular myocardium in 3 subsequent sections of E14.5 thorax running through the AV junction with a four chamber view from 5 embryos from 3 litters/each group. The values represent means ± STDEV. *, $P < 0.05$, **, $P < 0.01$; one-way ANOVA (brackets at top) with Bonferroni's multiple comparison post-test.

are thought to increase surface area to maximize oxygen uptake by the myocardium, our results are consistent with the hypothesis that the diabetic embryonic environment impairs tissue oxygen availability and may activate compensatory mechanisms to satisfy oxygen demands.

To investigate the mechanistic bases for the observed thin-walled myocardium, we quantified proliferation and apoptosis in the compact myocardium in both ventricles at E14.5. Isolated TUNEL-positive cells were seen in the endocardium, mesenchymal tissues of the forming cardiac skeleton, remodeling AV and outflow tract valves, and the interventricular septum of control embryos. A higher frequency of apoptotic cells was detected, mainly in the endocardial cushions and AV septum, of diabetes-exposed embryos. Since the majority of heart defects observed in diabetes-exposed embryos were AVS defects, we also analyzed apoptosis specifically in hearts with AVS defects. We detected a significant increase in apoptotic cells in *Hif1a*$^{+/-}$ diabetes-exposed embryos with AVS defects compared to *Hif1a*$^{+/-}$ embryos from non-diabetic pregnancies (Fig. 4; one-way ANOVA, $P < 0.02$).

Since the LV myocardial volume of diabetes-exposed *Hif1a*$^{+/-}$ embryos was significantly decreased compared to *Wt* littermates, we quantified cell proliferation by immunostaining for pHH3 at E10.5, and from E12.5 to E14.5 (Fig. 5). Mitotic activity was significantly decreased in the compact myocardium of diabetic hearts relative to the non-diabetic hearts at E10.5 and E12.5 (Figs. 5E–F). These data are consistent with previously published results [6,7] and suggest that the

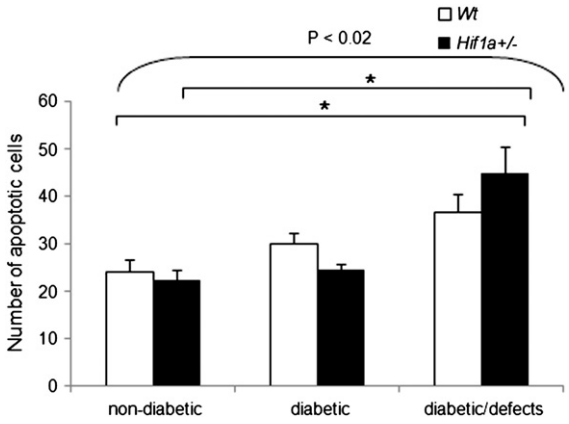

Fig. 4. Apoptosis in the diabetes-exposed and non-diabetic hearts of E14.5 *Wt* and *Hif1a*$^{+/-}$ embryos. The quantitative analysis showed that the number of apoptotic cells was significantly increased in *Hif1a*$^{+/-}$ diabetes-exposed embryos with heart defects compared to hearts from non-diabetic pregnancies (n = 3 embryos for each group and 3 slides/embryo). The values represent means ± STDEV. *, $P < 0.05$, one-way ANOVA (brackets at top) with Bonferroni's multiple comparison post-test.

formation of a thin myocardium in diabetes-exposed hearts is the result of decreased cell proliferation. Importantly, our analysis revealed a marked decrease in mitotic activity in the LV compact myocardium of *Hif1a*$^{+/-}$ diabetes-exposed hearts compared to *Wt* littermates at E12.5, E13.5, and E14.5 (Figs. 5F–H). Thus, cell proliferation in the LV compact myocardium of diabetes-exposed *Hif1a*$^{+/-}$ embryos is considerably reduced, which represents a cellular mechanism for the decreased volume of the LV compact myocardium in diabetic *Hif1a*$^{+/-}$ embryos.

3.3. Analysis of HIF-1α protein levels

To understand the basis for the escalation of congenital defects in *Hif1a*$^{+/-}$ diabetic embryos, we analyzed HIF-1α protein levels. Protein lysates were prepared from *Wt* and *Hif1a*$^{+/-}$ whole embryos and hearts at E10.5 (Fig. 6). Quantitative Western blot analysis showed significantly decreased HIF-1α levels in whole *Hif1a*$^{+/-}$ embryos by 1.9 fold relative to *Wt* embryos. In contrast, HIF-1α protein levels in the hearts of *Wt* and *Hif1a*$^{+/-}$ littermates from non-diabetic pregnancies were similar. HIF-1α levels were increased 2.9-fold in diabetes-exposed *Wt* hearts but only 1.8 fold in *Hif1a*$^{+/-}$ hearts, compared to non-diabetic *Wt* hearts.

3.4. Analysis of cardiac VEGF-A and α-SMA expression

Next, we focused on cardiac expression of VEGF-A, a key HIF-1 target gene product. VEGF-A is an essential modulator of cardiovascular development and modest increases or decreases in VEGF-A levels lead to embryonic lethality [37,38]. We analyzed histological sections of E14.5 hearts to establish the spatial expression of VEGF-A using immunohistochemistry. VEGF-A was detected in the interventricular septum, myocardial cells lining the endocardial cushions of both the inflow tract and the outflow tract, and in the ventricular myocardium (Figs. 7A–F). Diabetes significantly increased VEGF-A protein levels in *Wt* hearts but not in *Hif1a*$^{+/-}$ hearts (Fig. 7G). In diabetes-exposed *Hif1a*$^{+/-}$ hearts, the expression of VEGF-A was decreased in three of four analyzed embryos. We also used RT-qPCR to analyze *Vegfa* mRNA levels in the embryonic hearts at E14.5 (Fig. 7H). We detected a marked variability in *Vegfa* mRNA expression levels in the diabetes-exposed hearts. However, mean *Vegfa* mRNA levels in the hearts of diabetes-exposed *Hif1a*$^{+/-}$ embryos were markedly reduced compared to *Wt* littermates.

To further elucidate the roles of HIF-1α in cardiac responses to the diabetic environment, we analyzed spatial expression of α-SMA, a marker of immature cardiomyocytes. The expression of α-SMA in early cardiomyocytes is more prominent before E12.5 and its expression is decreased with cardiomyocyte maturation at E14.5 [39]. We observed a reduced number of α-SMA^{+} cardiomyocytes in both the LV and RV of diabetic *Hif1a*$^{+/-}$ embryos compared to non-diabetic embryos at E14.5 (Figs. 8A–B). Although the RV myocardial volume in diabetes-exposed *Wt* embryos was significantly decreased compared to non-diabetic *Wt* embryos (Fig. 3), the expression of α-SMA was similar in diabetic and non-diabetic RVs. Since mature cardiomyocytes lose α-SMA expression, the differences in the number of α-SMA^{+} cardiomyocytes may indicate dysregulated differentiation (maturation) of the ventricular cardiomyocytes in diabetic embryos.

3.5. Analysis of cardiac gene transcription

RT-qPCR was performed to analyze the expression of genes encoding molecules important for myofibrillogenesis, transcriptional regulation, differentiation, and proliferation, including T-box 5 (*Tbx5*), NK class homeodomain protein (*Nkx2.5*), atrial natriuretic peptide (*Nppa*), gap-junction gene connexin 43 (*Cx43*), myocyte enhancer factor 2C (*Mef2c*), skeletal α-actin 1 (*Acta1*), myosin light chain isoform (*Mlc2v*), and cardiac troponin I (*Tnni3*). Whereas expression of *Tbx5* was significantly decreased in non-diabetic *Hif1a*$^{+/-}$ compared to *Wt* hearts, it was markedly increased in diabetes-exposed *Hif1a*$^{+/-}$ hearts compared to non-diabetic and diabetic *Wt* hearts (Fig. 9). Expression of the cardiogenic factor *Nkx2.5* mRNA expression was also significantly increased in diabetes-exposed *Hif1a*$^{+/-}$ hearts. TBX5 and NKX2.5 can synergistically activate the *Nppa* gene promoter [40,41]. Expression levels of *Nppa* were significantly increased in diabetes-exposed *Hif1a*$^{+/-}$ embryos in accordance with the expression patterns of *Tbx5* and *Nkx2.5*. Next, we analyzed the expression of *Mef2c*, which encodes another cardiac-specific transcription factor. *Mef2c* mRNA levels were also increased in diabetes-exposed *Hif1a*$^{+/-}$ hearts but not in diabetes-exposed *Wt* hearts at E14.5. In contrast, maternal diabetes modestly increased the expression of a marker of myocardial cell differentiation, *Cx43*, in both *Wt* and *Hif1a*$^{+/-}$ hearts. The expression of *Acta1* was modestly decreased in both the *Wt* and *Hif1a*$^{+/-}$ diabetes-exposed hearts compared to non-diabetic hearts. The expression of myofilament genes, *Tnni3* and ventricle-specific *Mlc2v*, was not significantly affected by *Hif1a* genotype or the diabetic environment. Taken together, our data are consistent with the hypothesis that dysregulated gene expression in the hearts of *Hif1a*$^{+/-}$ embryos subjected to the diabetic environment underlies the increased incidence of congenital cardiac defects in these embryos.

4. Discussion

The teratogenic process in diabetic pregnancy is multifactorial. It is associated with numerous disturbances in embryonic development and growth and with compromised placental function. In this study, we have analyzed the effects of global heterozygous deletion of *Hif1a* on the embryonic response to maternal diabetes. Our study revealed that compared to *Wt* littermates, mouse embryos heterozygous for a knockout allele at the *Hif1a* locus have a decreased number of embryos per litter and increased incidence of malformations in the teratogenic environment of maternal diabetes. Previous studies have documented that embryos with the global knockout of *Hif1a* gene die by E10.5 displaying severe cardiovascular and neural tube defects [23,24]. In contrast, a cardiac myocyte-specific deletion of *Hif1a* is not lethal and does not cause an increased incidence of developmental cardiac defects [42]. Although in this study, we observed that cardiovascular defects were the most frequent defects in *Hif1a*$^{+/-}$ embryos from diabetic pregnancies, we cannot determine which cell type or which combinations of cell types are contributing to the increased susceptibility of *Hif1a*$^{+/-}$ mice to diabetic embryopathy due to the global nature of the *Hif1a* deletion. At the same time, the global deletion of *Hif1a* may additionally affect gene regulation in the embryonic

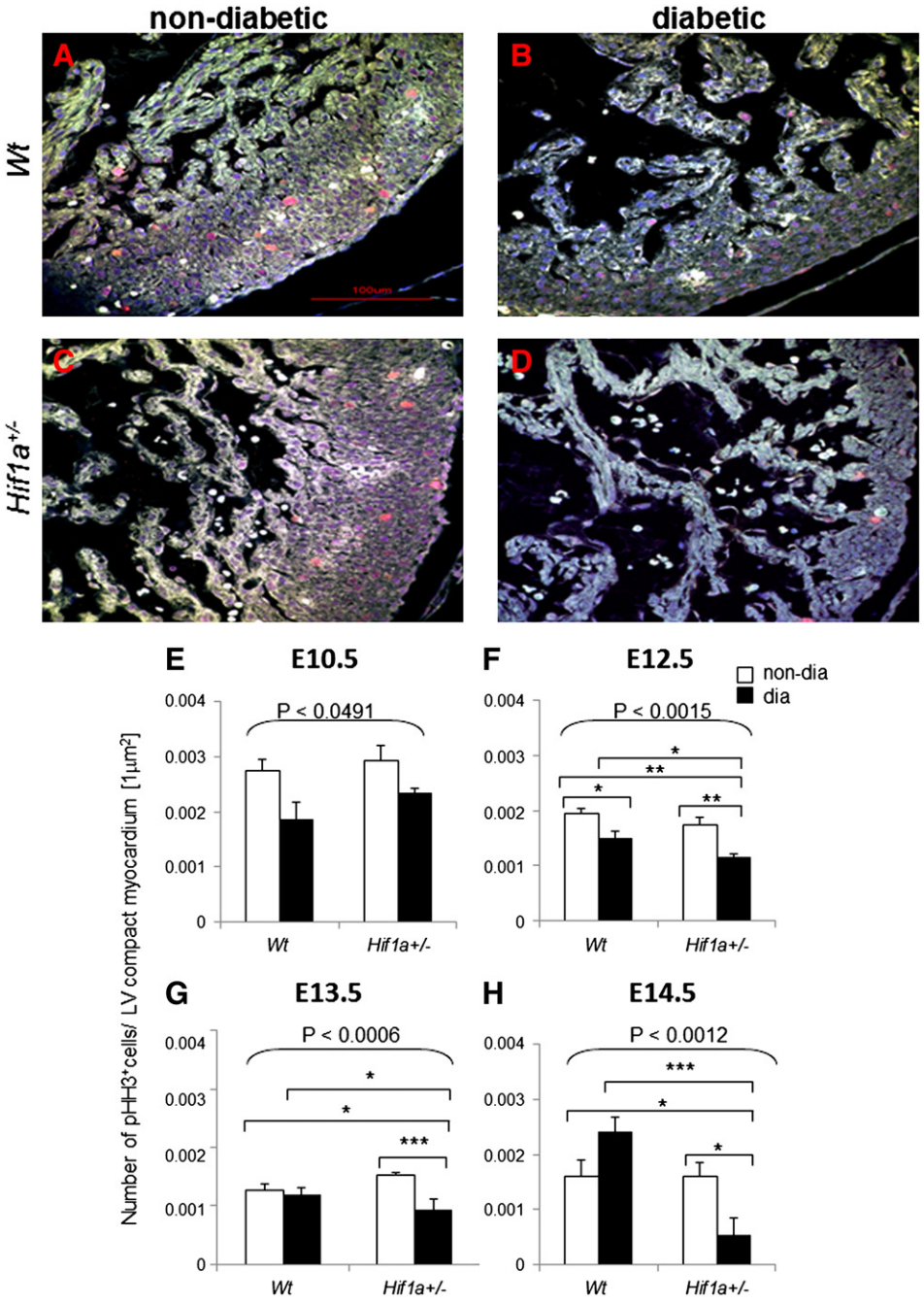

Fig. 5. Quantification of cellular proliferation in compact myocardium of the left ventricle of the diabetes-exposed and non-diabetic hearts of *Wt* and *Hif1a*$^{+/-}$ embryos. Heart sections (7 μm) were immunostained for phospho-histone H3 (pHH3) to detect mitotic cells in the compact myocardium at E10.5, E12.5, E13.5, and E14.5 (3 embryos per each group and 2–3 slides per embryo). Confocal imaging of transverse sections of the embryonic heart of stage E14.5 (green autofluorescence) stained with anti-pHH3 antibody (red) showed mitotic cells in the left ventricle of non-diabetic *Wt* (A) and *Hif1a*$^{+/-}$ (C), and diabetes-exposed *Wt* (B) and *Hif1a*$^{+/-}$ (D) embryos. Hoechst 33342 (blue) was used as a nuclear counterstain. Images are stacked Z-plane sections from confocal microscopy. Scale bar: 0.1 mm. (E–H) Quantification of pHH3^{+} cells was determined as an average pHH3^{+} nuclei per total tissue area of the left ventricular compact myocardium of the field using ImageJ software. The values represent means of number pHH3^{+} nuclei/μm^2 of left ventricular compact layer ± SEM. $^{*}P < 0.05$, $^{**}P < 0.01$, $^{***}P < 0.001$; one-way ANOVA (brackets at top) followed by post-*t*-test. LV, left ventricle.

compartments of the diabetic placenta. It can also contribute to placental dysfunction and to an overt pathological response in diabetic pregnancy.

In the present study, we have demonstrated increased HIF-1α levels in diabetes-exposed hearts compared to non-diabetic hearts at E10.5. Additionally, cardiac HIF-1α levels were reduced by 40% in diabetes-exposed hearts from *Hif1a*$^{+/-}$ embryos compared to *Wt* littermates, reflecting *Hif1a* haploinsufficiency. These differences in cardiac HIF-1α levels are evidence of differential responses between *Wt* and *Hif1a*$^{+/-}$ diabetes-exposed hearts. Under normoglycemic conditions, compensation for heterozygosity for the *Hif1a* knockout allele occurs, presumably by changes in the rate of synthesis or degradation of HIF-1α mRNA or protein. As a result, HIF-1α protein levels are not significantly decreased in the hearts of *Hif1a*$^{+/-}$ embryos and development proceeds normally. However, under the stress of maternal hyperglycemia, the adaptive increase in HIF-1α protein levels that is observed in *Wt* embryos cannot be achieved in *Hif1a*$^{+/-}$ embryos, thereby increasing their risk for congenital heart defects.

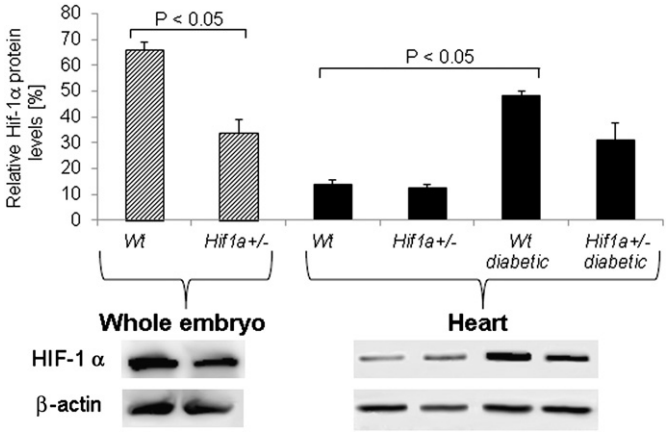

Fig. 6. Protein levels of HIF-1α. Western blot analysis of protein levels of HIF-1α in whole embryos and hearts at E10.5. HIF-1α protein levels were assessed by immunoblotting of total protein lysates (n = 2/whole embryos, diabetic hearts; n = 8/non-diabetic *Wt* hearts; and n = 10/non-diabetic *Hif1a*$^{+/-}$ hearts). A representative immunoblot is shown. HIF-1α protein levels were normalized to the expression of β-actin. Values are shown as a percentage of β-actin levels ± SEM. *$P < 0.05$; one-way ANOVA followed by Dunnett's post-test (all groups vs. non-diabetic *Wt*).

Interestingly, we found that the LV myocardial volume in diabetes-exposed *Hif1a*$^{+/-}$ hearts was significantly reduced compared to *Wt* littermates at E14.5. We detected significantly increased expression of *Tbx5* in diabetes-exposed *Hif1a*$^{+/-}$ hearts compared to *Wt* littermates that may play a major role in the pathogenesis of reduced LV myocardial volume. TBX5 is one of the important cardiac factors with distinct asymmetric expression, specifying the identity of the LV [43,44]. Existing evidence supports the role of TBX5 as a regulator of myocardial cell proliferation. Overexpression of *Tbx5* in embryonic chick heart inhibits myocardial cell proliferation [45]. Similarly, ubiquitous dysregulated expression of *Tbx5* in the embryonic heart is associated with a thinner ventricular wall compared to the normal heart [46]. TBX5 activates the *Nkx2.5* gene [40,41,46]. Additionally, TBX5 and NKX2.5 synergistically activate the *Nppa* gene [40]. Accordingly, we detected an increased expression of *Nkx2.5* and *Nppa* in the hearts of diabetes-exposed *Hif1a*$^{+/-}$ embryos but not *Wt* embryos at E14.5. *Nppa* is also specifically expressed in the LV but not in the RV in mid-gestation similar to *Tbx5* [57]. Existing evidence strongly suggests that the levels of *Tbx5* expression in the developing heart are crucial. Overexpression of *Tbx5* in the heart is associated with abnormalities of early chamber development, hypoplasia, loss of ventricular-specific gene expression, and embryonic lethality [45,58]. Similarly, homozygous *Tbx5*$^{-/-}$ mutants demonstrate the arrest in heart development at E9.5. Heterozygous *Tbx5*$^{+/-}$ mice show the congenital defects, including cardiac hypoplasia, atrial and ventricular septal defects, of Holt–Oram syndrome mutations in humans [40]. NKX2.5 mutations in humans are also associated with congenital heart defects similar to Holt–Oram syndrome [59]. Based on our results, we propose that the diabetic environment affects HIF-1α regulation in the developing heart and that haploinsufficiency of *Hif1a* alters compensatory mechanisms involving key transcriptional factors that regulate cardiac differentiation, morphogenesis, and growth.

Although hypoplasia of the heart ventricles was observed in all diabetes-exposed embryos, we did not detect a significant increase in apoptotic cells at E14.5. However, a statistically significant increase in the number of apoptotic cells was detected in *Hif1a*$^{+/-}$ hearts with AVS defects. Increased apoptosis in the cardiac cushions in pre-septation stages was associated with subsequent defects of cardiac septation in TGF-β2-deficient mice [47]. Our findings of increased apoptosis at the stage where the defects are already established may reflect either a persistence of the apoptotic stimulus or abnormal hemodynamic conditions in the malformed heart, which can also lead to apoptosis [48]. However, the majority of apoptotic cells in both malformed and normal hearts were found in physiological zones of programmed cell death associated with heart morphogenesis [49], specifically the mesenchymal cushions, valves, and interventricular septum, rather than in the myocardium of the free ventricular wall. These observations suggest that ventricular wall mass was not reduced because of increased apoptosis and are consistent with other studies, which have implicated decreased cell proliferation in the ventricular myocardium as the cause of hypoplastic myocardium in diabetes-exposed hearts [6,7]. The proliferation of cardiomyocytes is necessary to support the increasing hemodynamic load at mid-gestation [50]. During normal heart development, the number of cardiomyocytes in the compact layer of the ventricles increases 5-fold between E12.5 and E14.5 [51]. Previous work has associated decreased proliferation with the formation of a thin myocardium in diabetes-exposed hearts [6,7,52]. Consistent with these results, we observed significantly decreased mitotic activity in the compact myocardium of E10.5 and E12.5 diabetes-exposed embryos compared to non-diabetic embryos. Interestingly, we detected substantially reduced proliferation in the compact myocardium of the left ventricle in diabetes-exposed *Hif1a*$^{+/-}$ embryos compared to *Wt* littermates (Fig. 5), which corresponded to the more profound phenotype of thin ventricular compact myocardium and to the increased expression of *Tbx5*, an inhibitor of cardiomyocyte proliferation [45]. Moderately elevated mitotic activity in the compact myocardium of E14.5 diabetes-exposed *Wt* embryos suggests compensatory responses to the teratogenic diabetic environment. These different cellular responses between diabetes-exposed *Wt* and *Hif1a*$^{+/-}$ embryos may contribute to increase susceptibility to diabetic embryopathy in *Hif1a*$^{+/-}$ embryos. In contrast to morphological changes in the ventricular myocardium, the epicardium of diabetes-exposed hearts was characteristically spread over the myocardium, without any signs of detachment or blebbing. Since epicardial–myocardial interactions regulate differentiation and proliferation of the ventricular wall, the possibility that epicardium-mediated signals are altered in diabetes-exposed embryos remains to be determined.

Our data demonstrate that, compared to *Wt* embryos, *Hif1a*$^{+/-}$ littermates from diabetic pregnancies with moderate hyperglycemia are more susceptible to diabetic embryopathy. To further evaluate the role of HIF-1-regulated pathways in diabetic embryopathy, we analyzed the expression of a key HIF-1 target gene, *Vegfa*, which is tightly regulated during normal embryonic development. Heterozygous *Vegfa*$^{+/-}$ mutant embryos die at E10.5, displaying abnormal vascularization. Transgenic embryos overexpressing VEGF-A also die with severe cardiac abnormalities at E12.5–E14 [37,38,53]. Our previous research has demonstrated that the expression of *Vegfa* is altered by the diabetic environment at E10.5 [17]. Cultured mouse embryos exposed to high glucose from E7.5 until E9.5 showed a reduction in VEGF-A levels and significant vascular abnormalities [54]. A decrease in *Vegfa* mRNA was observed in the hearts of E14 rat embryos (corresponding to E12.5 in the mouse) from diabetic pregnancies, although 25% of the analyzed embryos were not affected by the diabetic environment [55]. In contrast, an increased expression of *Vegfa* mRNA and VEGF-A protein was detected in the hearts of E13.5 mouse embryos from diabetic pregnancies [56]. In the present study, VEGF-A levels were on average increased in *Wt* but not *Hif1a*$^{+/-}$ embryos at E14.5. Our RT-qPCR analysis showed a high variability in *Vegfa* mRNA levels with a prevailing trend of decreased *Vegfa* expression in *Hif1a*$^{+/-}$ diabetes-exposed embryos at E14.5, supporting the idea of altered HIF-1 regulation that may increase the risk of cardiac malformations in *Hif1a*$^{+/-}$ embryos.

Maternal-diabetes-induced specific morphogenetic defects represent a phenotype of incomplete penetrance. A recently proposed explanation of the etiology of diabetic embryopathy based on gene expression highlighted two components, the deregulation of gene expression and increased variability of gene expression [60]. In our case, *Hif1a*$^{+/-}$ genotype and an increased variability of gene expression produce discrete differences among embryos, which can trigger pathogenic events resulting in congenital defects.

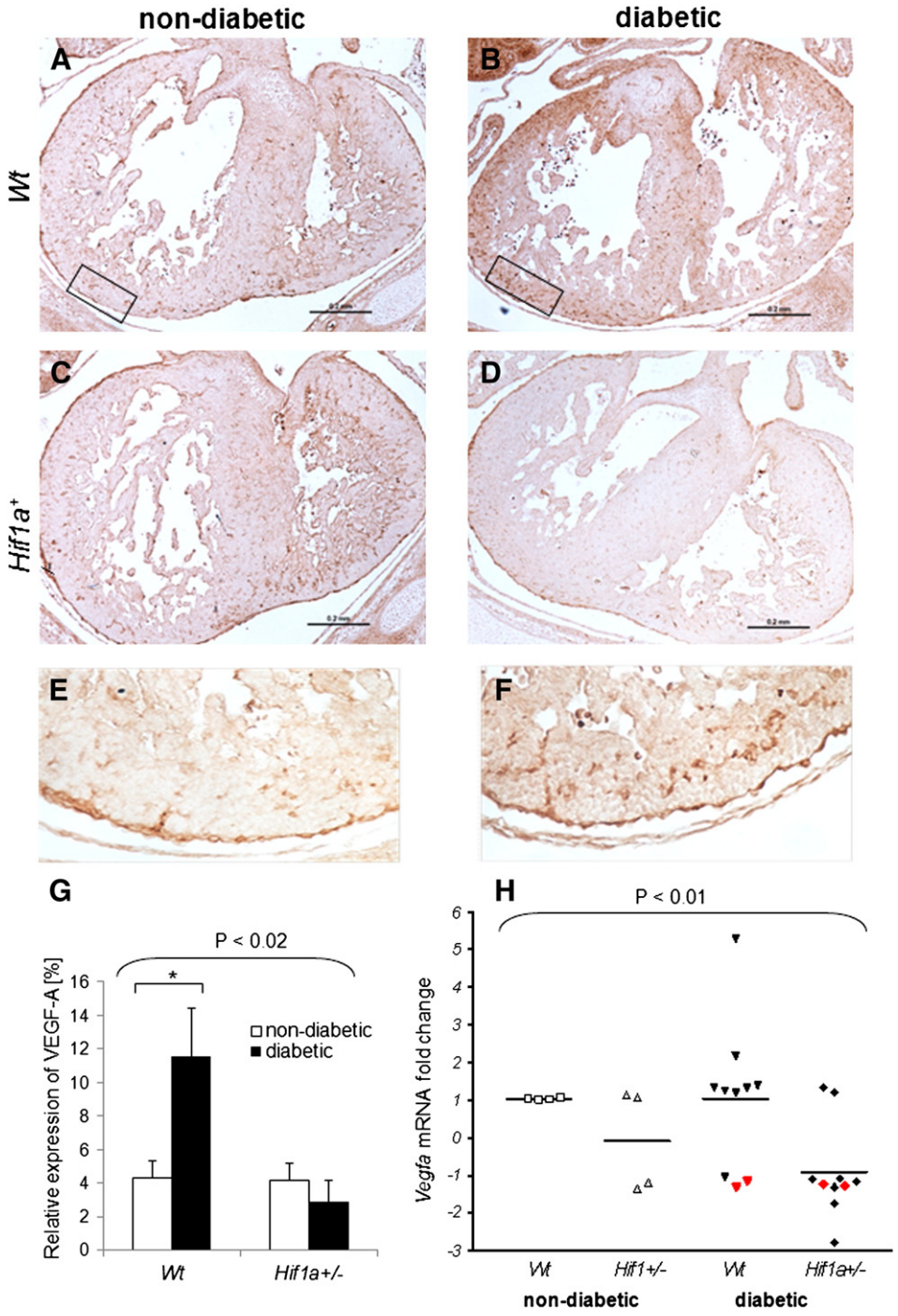

Fig. 7. Diabetes-induced increase in cardiac VEGF expression. In the E14.5 heart, a diabetes-induced increase in VEGF-A expression was detected in all myocardial cells aligning the endocardial cushions of both the inflow tract and the outflow tract of the heart, in the interventricular septum, and in the ventricular myocardium of embryos. Transverse sections of embryos stained with anti-VEGF-A antibody showed increased VEGF-A expression in two of four *Wt* analyzed embryos compared to non-diabetic controls (A, B). In diabetes-exposed *Hif1a*$^{+/-}$ hearts, the expression of VEGF-A was decreased in three of four analyzed embryos (C, D). (A–D): overview Scale bar: 0.2 mm, original magnification 10×. Boxed areas are shown at higher magnification, (E) non-diabetic *Wt* and (F) diabetic *Wt* (original magnification 40×). IVS, interventricular septum; LV, left ventricle; RA, right atrium; RV, right ventricle. (G) Quantification of VEGF-A stained area was determined as a percentage of total tissue area of the interventricular septum and LV myocardium of the field using ImageJ software. The values represent means ± STDEV (n = 4 embryos/group). Differences in VEGF-A expression were significant between diabetic *Wt* and non-diabetic *Wt* hearts. Statistical significance was assessed by one-way ANOVA (brackets at top). *, $P < 0.05$ (Dunnett's post-test). (H) RT-qPCR analysis of expression of *Vegfa* mRNA in *Wt* and *Hif1a*$^{+/-}$ hearts from diabetic and normal pregnancies at E14.5. The relative expression levels were quantified using ΔΔCT method. The data represent an expression of mRNA relative to non-diabetic *Wt* expression of mRNA, normalized by the housekeeping mRNA of *Hprt1*. Differences in normalized Ct values *Wt* and *Hif1a*$^{+/-}$ from diabetic pregnancy, and non-diabetic *Hif1a*$^{+/-}$ were significant compared to non-diabetic *Wt* ($P < 0.01$, one-way ANOVA). The relative expression of *Vegfa* for each individual embryo is shown. Two *Wt* and *Hif1a*$^{+/-}$ embryos from diabetic pregnancies with severe hyperglycemia were included into the analysis (red). Horizontal bars represent average expression of *Vegfa* for each group.

Studies in adult mice have demonstrated that HIF-1-dependent vascularization following femoral artery ligation or cutaneous wounding is impaired in diabetic mice, which can be rescued by experimental manipulations that increase HIF-1α expression [61–63]. Loss of HIF-1 activity appears to play a role in the pathogenesis of type 2 diabetes [64,65]. Thus, environmental (maternal diabetes) and genetic (*Hif1a* mutation)

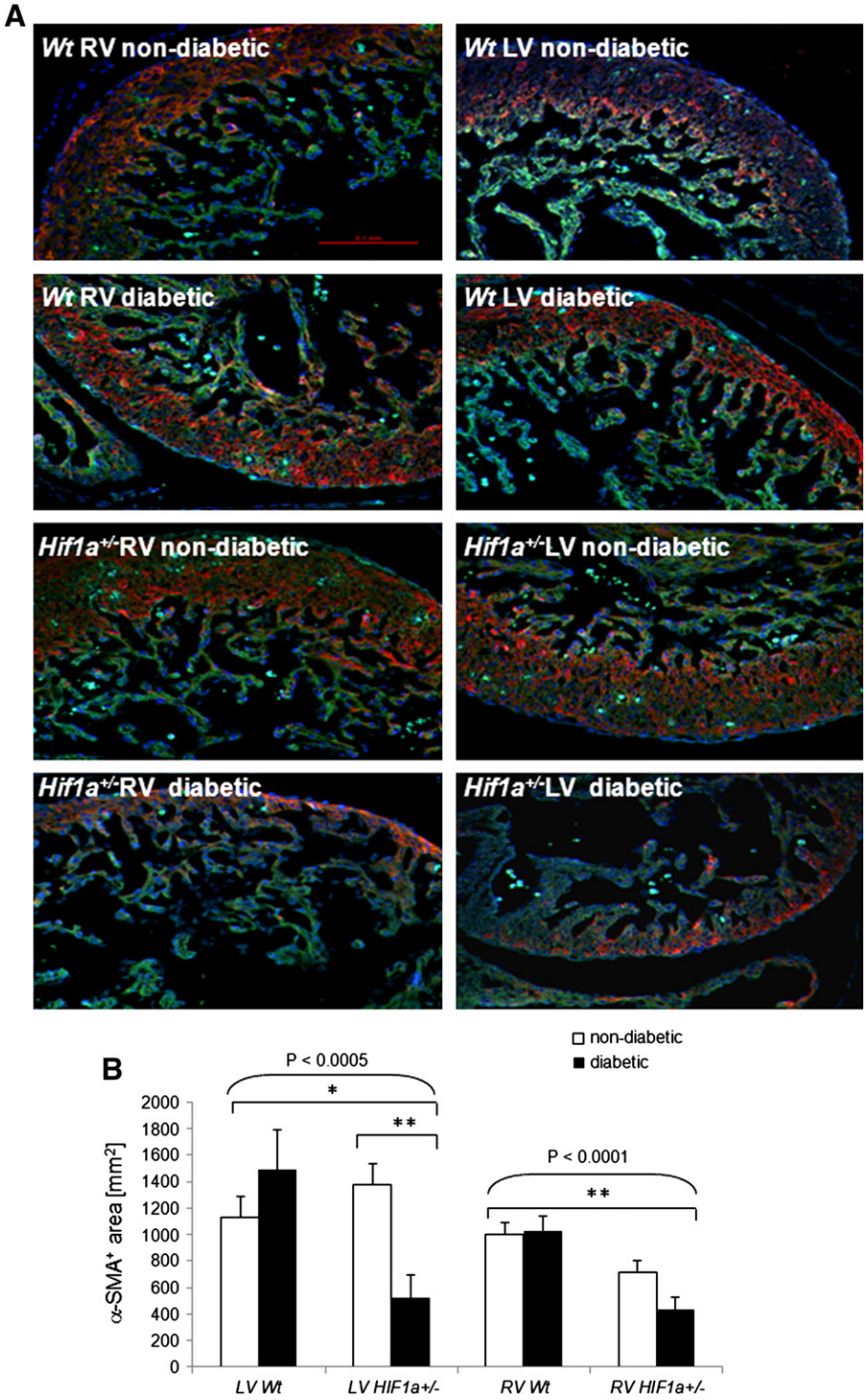

Fig. 8. Diabetes-induced changes in the ventricular myocardium. (A) Confocal imaging of transverse sections of embryonic heart of stage E14.5 (green autofluorescence) stained with anti-α-SMA antibody (red) showed hypoplasia of the compact ventricular myocardium in both *Wt* and *Hif1a*$^{+/-}$ diabetes-exposed embryos. Hoechst 33342 (blue) was used as a nuclear counterstain. Images are stacked Z-plane sections from confocal microscopy. LV, left ventricle; RV, right ventricle. Scale bar: 0.1 mm. (B) Relative quantification of α-SMA^{+} area per field is shown. Quantification of α-SMA^{+} area was determined as a percentage of total tissue area of the field of view using ImageJ software. Statistical significance was assessed by one-way ANOVA with Dunnett's post-test (all groups vs. non-diabetic *Wt*). The values represent means ± SEM (n = 4 embryos from 3 litters/group). *, $P < 0.05$, **, $P < 0.01$.

factors may each reduce HIF-1 activity in embryos and result in congenital malformations if either abnormality is severe enough (i.e. maternal blood glucose > 30 mmol/L *or Hif1a*$^{-/-}$ genotype) or when more modest abnormalities are present in combination (i.e. maternal blood glucose between 13.9 and 30 mmol/L *and Hif1a*$^{+/-}$ genotype). Furthermore, clinical studies have associated a loss of gene copy of *HIF1A* with ventricular septal defects [66]. Taken together with the results presented here, these data raise the possibility that genetic variation at the *HIF1A* locus may influence malformation risk for infants of diabetic mothers.

5. Conclusions

We used a genetic mouse model of partial global HIF-1α deficiency to test our hypothesis that induction of HIF-1α represents one of the

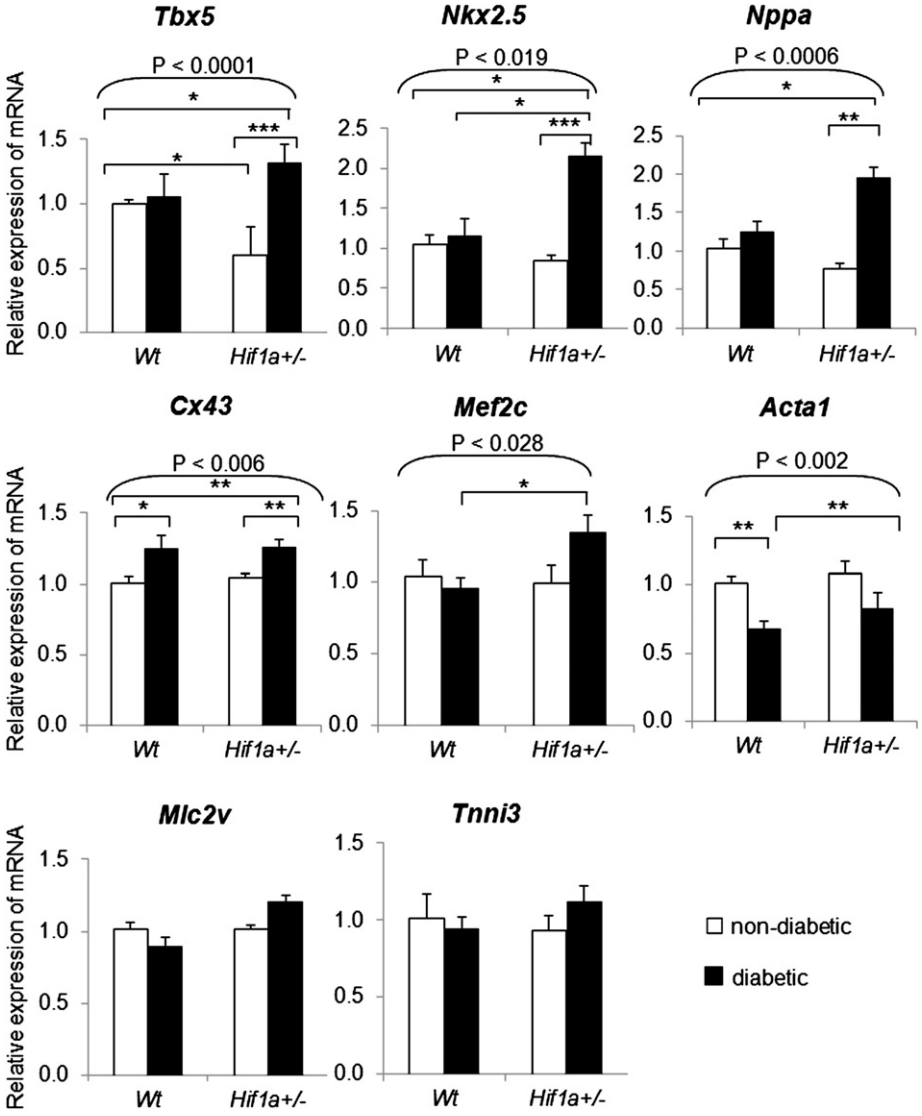

Fig. 9. Gene expression changes in *Wt* and *Hif1a*$^{+/-}$ hearts exposed to maternal diabetes at E14.5. The expression of selected genes was analyzed using RT-qPCR. The relative expression levels were quantified using ΔΔCT method. The data represent an expression of mRNA relative to non-diabetic *Wt* expression of mRNA, normalized by the housekeeping mRNA of *Hprt1*. The values represent means ± SEM (each experiment in duplicate; n = 8 per groups of diabetic *Wt* and *Hif1a*$^{+/-}$, non-diabetic *Hif1a*$^{+/-}$; n = 6 per non-diabetic *Wt*). Differences in normalized Ct values were tested for statistical significance by one-way ANOVA (brackets at top) followed by Bonferroni's multiple comparison post-test. *, $P < 0.05$, **, $P < 0.01$, ***, $P < 0.001$.

adaptive responses to maternal diabetes and that a failure to adequately induce expression of HIF-1α increases susceptibility to diabetic embryopathy. HIF-1α heterozygous-null and *Wt* littermate embryos were exposed to the intrauterine environment of a diabetic mother and the frequency and morphology of heart defects were analyzed. We found that the global reduction in functional *Hif1a* gene dosage decreased the number of embryos per litter and increased the incidence of heart malformations, mainly AVS defects and reduced ventricular myocardial mass, in diabetes-exposed *Hif1a*$^{+/-}$ compared to *Wt* littermates. We also detected significant changes in the expression of *Vegfa* and key cardiogenic transcription factors *Tbx5*, *Nkx2.5*, and *Mef2c* in diabetes-exposed *Hif1a*$^{+/-}$ compared to *Wt* embryonic hearts. These changes provide a molecular mechanism by which HIF-1α loss-of-function may increase the risk of congenital malformations. Taken together, these results are compelling evidence that impairment of HIF-1α-controlled hypoxia-response pathways may play a functionally causative role in diabetic embryopathy.

Supplementary data to this article can be found online at http://dx.doi.org/10.1016/j.yjmcc.2013.04.015.

Funding sources

This work was funded by a Marie Curie International Reintegration Grant within the 7th European Community Framework Programme PIRG02-GA-2007-224760; grants from the Czech Ministry of Education, Youth and Sports AVOZ50520701; and the Czech Science Foundation 301/09/0117 and 302/11/1308.

Disclosure statement

None declared.

Acknowledgments

G.L.S. is the C. Michael Armstrong Professor at the Johns Hopkins University School of Medicine. Dr. Gabriela Pavlinkova is the guarantor of this work, had full access to all the data, and takes full responsibility for the integrity of data and the accuracy of data analysis. R.B., L.K. collected and analyzed the data. G.P. analyzed the data, wrote and

reviewed the manuscript. D.S. analyzed the data, contributed to the discussion, and edited the manuscript. G.L.S. contributed to the discussion, reviewed and edited the manuscript. We also thank J. Truksa (Institute of Biotechnology AS CR) for help with Western blot analysis.

References

[1] Martinez-Frias ML. Epidemiological analysis of outcomes of pregnancy in diabetic mothers: identification of the most characteristic and most frequent congenital anomalies. Am J Med Genet 1994;51:108–13.
[2] Kucera J. Rate and type of congenital anomalies among offspring of diabetic women. J Reprod Med 1971;7:73–82.
[3] Wren C, Birrell G, Hawthorne G. Cardiovascular malformations in infants of diabetic mothers. Heart 2003;89:1217–20.
[4] Corrigan N, Brazil DP, McAuliffe F. Fetal cardiac effects of maternal hyperglycemia during pregnancy. Birth Defects Res A Clin Mol Teratol 2009;85:523–30.
[5] Correa A, Gilboa SM, Besser LM, Botto LD, Moore CA, Hobbs CA, et al. Diabetes mellitus and birth defects.Am J Obstet Gynecol 2008;199:237 [e1-9].
[6] Kumar SD, Dheen ST, Tay SS. Maternal diabetes induces congenital heart defects in mice by altering the expression of genes involved in cardiovascular development. Cardiovasc Diabetol 2007;6:34.
[7] Zhao Z. Cardiac malformations and alteration of TGFbeta signaling system in diabetic embryopathy. Birth Defects Res B Dev Reprod Toxicol 2010;89:97–105.
[8] Molin DG, Roest PA, Nordstrand H, Wisse LJ, Poelmann RE, Eriksson UJ, et al. Disturbed morphogenesis of cardiac outflow tract and increased rate of aortic arch anomalies in the offspring of diabetic rats. Birth Defects Res A Clin Mol Teratol 2004;70:927–38.
[9] Phelan SA, Ito M, Loeken MR. Neural tube defects in embryos of diabetic mice: role of the Pax-3 gene and apoptosis. Diabetes 1997;46:1189–97.
[10] Sussman I, Matschinsky FM. Diabetes affects sorbitol and myo-inositol levels of neuroectodermal tissue during embryogenesis in rat. Diabetes 1988;37:974–81.
[11] Reece EA, Homko CJ, Wu YK, Wiznitzer A. The role of free radicals and membrane lipids in diabetes-induced congenital malformations. J Soc Gynecol Investig 1998;5:178–87.
[12] Yang X, Borg LA, Eriksson UJ. Altered metabolism and superoxide generation in neural tissue of rat embryos exposed to high glucose. Am J Physiol 1997;272:E173–80.
[13] Sakamaki H, Akazawa S, Ishibashi M, Izumino K, Takino H, Yamasaki H, et al. Significance of glutathione-dependent antioxidant system in diabetes-induced embryonic malformations. Diabetes 1999;48:1138–44.
[14] Li R, Chase M, Jung SK, Smith PJ, Loeken MR. Hypoxic stress in diabetic pregnancy contributes to impaired embryo gene expression and defective development by inducing oxidative stress. Am J Physiol Endocrinol Metab 2005;289:E591–9.
[15] Wentzel P, Eriksson UJ. A diabetes-like environment increases malformation rate and diminishes prostaglandin E(2) in rat embryos: reversal by administration of vitamin E and folic acid. Birth Defects Res A Clin Mol Teratol 2005;73:506–11.
[16] Ornoy A. Embryonic oxidative stress as a mechanism of teratogenesis with special emphasis on diabetic embryopathy. Reprod Toxicol 2007;24:31–41.
[17] Pavlinkova G, Salbaum JM, Kappen C. Maternal diabetes alters transcriptional programs in the developing embryo. BMC Genomics 2009;10:274.
[18] Salbaum JM, Kruger C, Zhang X, Delahaye NA, Pavlinkova G, Burk DH, et al. Altered gene expression and spongiotrophoblast differentiation in placenta from a mouse model of diabetes in pregnancy. Diabetologia 2011;54:1909–20.
[19] Semenza GL. Oxygen sensing, homeostasis, and disease. N Engl J Med 2011;365:537–47.
[20] Bardos JI, Ashcroft M. Negative and positive regulation of HIF-1: a complex network. Biochim Biophys Acta 2005;1755:107–20.
[21] Haddad JJ, Harb HL. Cytokines and the regulation of hypoxia-inducible factor (HIF)-1alpha. Int Immunopharmacol 2005;5:461–83.
[22] Klimova T, Chandel NS. Mitochondrial complex III regulates hypoxic activation of HIF. Cell Death Differ 2008;15:660–6.
[23] Iyer NV, Kotch LE, Agani F, Leung SW, Laughner E, Wenger RH, et al. Cellular and developmental control of O_2 homeostasis by hypoxia-inducible factor 1 alpha. Genes Dev 1998;12:149–62.
[24] Kotch LE, Iyer NV, Laughner E, Semenza GL. Defective vascularization of HIF-1alpha-null embryos is not associated with VEGF deficiency but with mesenchymal cell death. Dev Biol 1999;209:254–67.
[25] Compernolle V, Brusselmans K, Franco D, Moorman A, Dewerchin M, Collen D, et al. Cardia bifida, defective heart development and abnormal neural crest migration in embryos lacking hypoxia-inducible factor-1alpha. Cardiovasc Res 2003;60:569–79.
[26] Krishnan J, Ahuja P, Bodenmann S, Knapik D, Perriard E, Krek W, et al. Essential role of developmentally activated hypoxia-inducible factor 1alpha for cardiac morphogenesis and function. Circ Res 2008;103:1139–46.
[27] Yin Z, Haynie J, Yang X, Han B, Kiatchoosakun S, Restivo J, et al. The essential role of Cited2, a negative regulator for HIF-1alpha, in heart development and neurulation. Proc Natl Acad Sci USA 2002;99:10488–93.
[28] Xu B, Doughman Y, Turakhia M, Jiang W, Landsettle CE, Agani FH, et al. Partial rescue of defects in Cited2-deficient embryos by HIF-1alpha heterozygosity. Dev Biol 2007;301:130–40.
[29] Wikenheiser J, Wolfram JA, Gargesha M, Yang K, Karunamuni G, Wilson DL, et al. Altered hypoxia-inducible factor-1 alpha expression levels correlate with coronary vessel anomalies. Dev Dyn 2009;238:2688–700.
[30] Kline DD, Peng YJ, Manalo DJ, Semenza GL, Prabhakar NR. Defective carotid body function and impaired ventilatory responses to chronic hypoxia in mice partially deficient for hypoxia-inducible factor 1 alpha. PNAS 2002;99:821–6.
[31] Li J, Bosch-Marce M, Nanayakkara A, Savransky V, Fried SK, Semenza GL, et al. Altered metabolic responses to intermittent hypoxia in mice with partial deficiency of hypoxia-inducible factor 1α. Physiol Genomics 2006;25:450–7.
[32] Zhang H, Bosch-Marce M, Shimoda LA, Tan YS, Baek JH, Wesley JB, et al. Mitochondrial autophagy is an HIF-1-dependent adaptive metabolic response to hypoxia. J Biol Chem 2008;283:10892–903.
[33] Peng YJ, Yuan G, Ramakrishnan D, Sharma SD, Bosch-Marce M, Kumar GK, et al. Heterozygous HIF-1alpha deficiency impairs carotid body-mediated systemic responses and reactive oxygen species generation in mice exposed to intermittent hypoxia. J Physiol 2006;577:705–16.
[34] Bohuslavova R, Kolar F, Kuthanova L, Neckar J, Tichopad A, Pavlinkova G. Gene expression profiling of sex differences in HIF1-dependent adaptive cardiac responses to chronic hypoxia. J Appl Physiol 2010;109:1195–202.
[35] Ream M, Ray AM, Chandra R, Chikaraishi DM. Early fetal hypoxia leads to growth restriction and myocardial thinning. Am J Physiol Regul Integr Comp Physiol 2008;295:R583–95.
[36] Pfaffl MW. A new mathematical model for relative quantification in real-time RT-PCR. Nucleic Acids Res 2001;29:e45.
[37] Carmeliet P, Ferreira V, Breier G, Pollefeyt S, Kieckens L, Gertsenstein M, et al. Abnormal blood vessel development and lethality in embryos lacking a single VEGF allele. Nature 1996;380:435–9.
[38] Miquerol L, Langille BL, Nagy A. Embryonic development is disrupted by modest increases in vascular endothelial growth factor gene expression. Development 2000;127:3941–6.
[39] Huang X, Gao X, Diaz-Trelles R, Ruiz-Lozano P, Wang Z. Coronary development is regulated by ATP-dependent SWI/SNF chromatin remodeling component BAF180. Dev Biol 2008;319:258–66.
[40] Bruneau BG, Nemer G, Schmitt JP, Charron F, Robitaille L, Caron S, et al. A murine model of Holt–Oram syndrome defines roles of the T-box transcription factor Tbx5 in cardiogenesis and disease. Cell 2001;106:709–21.
[41] Hiroi Y, Kudoh S, Monzen K, Ikeda Y, Yazaki Y, Nagai R, et al. Tbx5 associates with Nkx2–5 and synergistically promotes cardiomyocyte differentiation. Nat Genet 2001;28:276–80.
[42] Kuschel A, Simon P, Tug S. Functional regulation of HIF-1alpha under normoxia—is there more than post-translational regulation? J Cell Physiol 2012;227:514–24.
[43] Bruneau BG, Logan M, Davis N, Levi T, Tabin CJ, Seidman JG, et al. Chamber-specific cardiac expression of Tbx5 and heart defects in Holt–Oram syndrome. Dev Biol 1999;211:100–8.
[44] Takeuchi JK, Koshiba-Takeuchi K, Matsumoto K, Vogel-Hopker A, Naitoh-Matsuo M, Ogura K, et al. Tbx5 and Tbx4 genes determine the wing/leg identity of limb buds. Nature 1999;398:810–4.
[45] Hatcher CJ, Kim MS, Mah CS, Goldstein MM, Wong B, Mikawa T, et al. TBX5 transcription factor regulates cell proliferation during cardiogenesis. Dev Biol 2001;230:177–88.
[46] Takeuchi JK, Ohgi M, Koshiba-Takeuchi K, Shiratori H, Sakaki I, Ogura K, et al. Tbx5 specifies the left/right ventricles and ventricular septum position during cardiogenesis. Development 2003;130:5953–64.
[47] Kubalak SW, Hutson DR, Scott KK, Shannon RA. Elevated transforming growth factor beta2 enhances apoptosis and contributes to abnormal outflow tract and aortic sac development in retinoic X receptor alpha knockout embryos. Development 2002;129:733–46.
[48] Sedmera D, Hu N, Weiss KM, Keller BB, Denslow S, Thompson RP. Cellular changes in experimental left heart hypoplasia. Anat Rec 2002;267:137–45.
[49] Bartram U, Molin DG, Wisse LJ, Mohamad A, Sanford LP, Doetschman T, et al. Double-outlet right ventricle and overriding tricuspid valve reflect disturbances of looping, myocardialization, endocardial cushion differentiation, and apoptosis in TGF-beta(2)-knockout mice. Circulation 2001;103:2745–52.
[50] Srivastava D, Olson EN. A genetic blueprint for cardiac development. Nature 2000;407:221–6.
[51] Toyoda M, Shirato H, Nakajima K, Kojima M, Takahashi M, Kubota M, et al. Jumonji downregulates cardiac cell proliferation by repressing cyclin D1 expression. Dev Cell 2003;5:85–97.
[52] Gutierrez JC, Hrubec TC, Prater MR, Smith BJ, Freeman LE, Holladay SD. Aortic and ventricular dilation and myocardial reduction in gestation day 17 ICR mouse fetuses of diabetic mothers. Birth Defects Res A Clin Mol Teratol 2007;79:459–64.
[53] Dor Y, Camenisch TD, Itin A, Fishman GI, McDonald JA, Carmeliet P, et al. A novel role for VEGF in endocardial cushion formation and its potential contribution to congenital heart defects. Development 2001;128:1531–8.
[54] Pinter E, Haigh J, Nagy A, Madri JA. Hyperglycemia-induced vasculopathy in the murine conceptus is mediated via reductions of VEGF-A expression and VEGF receptor activation. Am J Pathol 2001;158:1199–206.
[55] Roest PA, Molin DG, Schalkwijk CG, van Iperen L, Wentzel P, Eriksson UJ, et al. Specific local cardiovascular changes of Nepsilon-(carboxymethyl)lysine, vascular endothelial growth factor, and Smad2 in the developing embryos coincide with maternal diabetes-induced congenital heart defects. Diabetes 2009;58:1222–8.
[56] Kumar SD, Yong SK, Dheen ST, Bay BH, Tay SS. Cardiac malformations are associated with altered expression of vascular endothelial growth factor and endothelial nitric oxide synthase genes in embryos of diabetic mice. Exp Biol Med (Maywood) 2008;233:1421–32.
[57] Zeller R, Bloch KD, Williams BS, Arceci RJ, Seidman CE. Localized expression of the atrial natriuretic factor gene during cardiac embryogenesis. Genes Dev 1987;1:693–8.
[58] Liberatore CM, Searcy-Schrick RD, Yutzey KE. Ventricular expression of tbx5 inhibits normal heart chamber development. Dev Biol 2000;223:169–80.

[59] Schott JJ, Benson DW, Basson CT, Pease W, Silberbach GM, Moak JP, et al. Congenital heart disease caused by mutations in the transcription factor NKX2-5. Science 1998;281:108–11.
[60] Salbaum JM, Kappen C. Diabetic embryopathy: a role for the epigenome? Birth Defects Res A Clin Mol Teratol 2011;91:770–80.
[61] Botusan IR, Sunkari VG, Savu O, Catrina AI, Grunler J, Lindberg S, et al. Stabilization of HIF-1alpha is critical to improve wound healing in diabetic mice. PNAS 2008;105:19426–31.
[62] Liu L, Marti GP, Wei X, Zhang X, Zhang H, Liu YV, et al. Age-dependent impairment of HIF-1alpha expression in diabetic mice: correction with electroporation-facilitated gene therapy increases wound healing, angiogenesis, and circulating angiogenic cells. J Cell Physiol 2008;217:319–27.
[63] Sarkar K, Fox-Talbot K, Steenbergen C, Bosch-Marce M, Semenza GL. Adenoviral transfer of HIF-1alpha enhances vascular responses to critical limb ischemia in diabetic mice. PNAS 2009;106:18769–74.
[64] Cheng K, Ho K, Stokes R, Scott C, Lau SM, Hawthorne WJ, et al. Hypoxia-inducible factor-1alpha regulates beta cell function in mouse and human islets. J Clin Invest 2010;120:2171–83.
[65] Gunton JE, Kulkarni RN, Yim S, Okada T, Hawthorne WJ, Tseng YH, et al. Loss of ARNT/HIF1beta mediates altered gene expression and pancreatic-islet dysfunction in human type 2 diabetes. Cell 2005;122:337–49.
[66] Lage K, Greenway SC, Rosenfeld JA, Wakimoto H, Gorham JM, Segre AV, et al. Genetic and environmental risk factors in congenital heart disease functionally converge in protein networks driving heart development. PNAS 2012;109:14035–40.